

THE BINDING OF THE ANTITUMOR ANTIBIOTIC CHARTREUSIN TO
POLY(dA-dT)·POLY(dA-dT), POLY(dG-dC)·POLY(dG-dC), CALF
THYMUS DNA, TRANSFER RNA, AND
RIBOSOMAL RNA

WILLIAM C. KRUEGER* and LORAIN M. PSCHIGODA

The Upjohn Company,
Kalamazoo, Michigan 49001, U.S.A.

ALBERT MOSCOWITZ

University of Minnesota,
Minneapolis, Minnesota 55455, U.S.A.

(Received for publication March 28, 1986)

Chartreusin binds cooperatively to poly(dA-dT)·poly(dA-dT) and poly(dG-dC)·poly(dG-dC). Both the site-exclusion model and the specific site model yield cooperative binding constants of about $5 \times 10^5 \text{ M}^{-1}$ and $3 \times 10^5 \text{ M}^{-1}$ for the AT and GC polymers, respectively, and the same stoichiometry and intrinsic binding constant for both polymers of 5 nucleotides per binding site and $3.1 \times 10^4 \text{ M}^{-1}$. The Scatchard plot for calf thymus DNA is curved in the opposite sense from that of cooperative binding. These binding data did not fit the site-exclusion model with the cooperative binding parameter as a variable nor the specific site, negative-cooperative binding model. The site-exclusion model with a cooperative binding parameter of unity yielded a binding constant of about $4 \times 10^4 \text{ M}^{-1}$ and a stoichiometry of about 5 nucleotides per binding site. The same model for transfer and ribosomal RNA yielded binding constants of $5 \times 10^3 \text{ M}^{-1}$ and $7 \times 10^3 \text{ M}^{-1}$ and stoichiometries of about 13 and 6 nucleotides per binding site, respectively.

Chartreusin is an antitumor antibiotic isolated from *Streptomyces chartreusis*.¹⁾ Its structure, Fig. 1, was determined by chemical degradation methods.²⁾ Chartreusin is active against a number of mouse tumors,^{3,4)} but was not developed clinically because of low solubility and rapid excretion into the bile. However, a biologically active analog of chartreusin that does not show low solubility or rapid excretion has recently been isolated.⁵⁾

Efforts to determine the mechanism of antitumor activity of chartreusin revealed that it inhibits RNA, DNA, and protein synthesis and RNA and DNA polymerase activities.⁶⁾ Chartreusin is known to induce DNA strand scission.⁷⁾ Furthermore, it was recently shown that chartreusin binds to DNA and inhibits relaxation of negatively superhelical DNA.⁸⁾ Qualitative interaction studies (absorbance and circular dichroism) carried out to determine the target biomolecule showed that chartreusin binds to calf thymus DNA (CT-DNA), poly(dA-dT)·poly(dA-dT), poly(dG-dC)·poly(dG-dC), and ribosomal RNA (r-RNA).⁶⁾ In this work, we present a quanti-

Fig. 1. Structure of chartreusin.

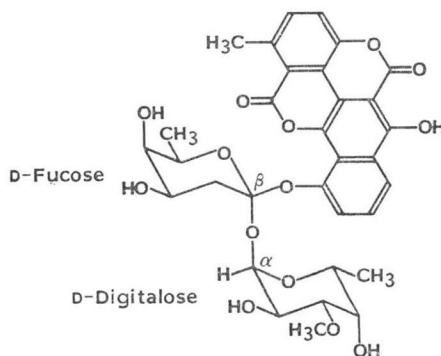
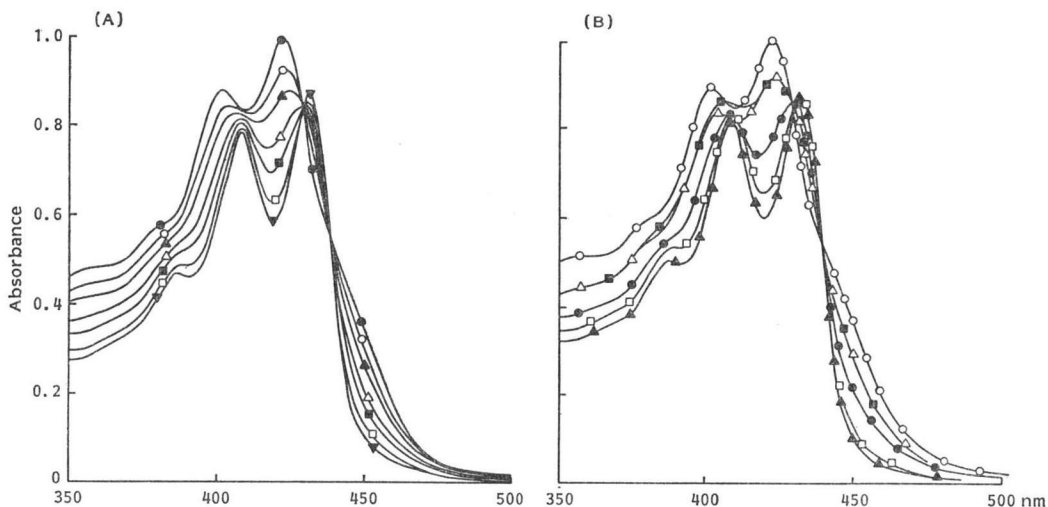


Fig. 2.

- (A) Change in the absorbance spectrum of chartreusin (1.6×10^{-5} M) with added CT-DNA. ● 0.0, ○ 1.6, ▲ 3.2, △ 6.3, ■ 9.2, □ 14.9, ▼ 34.9. The numbers give the molar ratio of nucleotide to chartreusin. 5 cm cell.
- (B) The effect of the biopolymers on the absorbance spectrum of chartreusin (1.6×10^{-5} M). 5 cm cell. The molar ratio of nucleotide to chartreusin is 6.5. ○ Chartreusin, △ t-RNA, ■ r-RNA, ● CT-DNA, □ GC polymer, ▲ AT polymer.



tative study of the binding of chartreusin to poly(dA-dT)·poly(dA-dT), poly(dG-dC)·poly(dG-dC), CT-DNA, transfer RNA (t-RNA) and r-RNA.

Materials and Methods

Escherichia coli 16s+23s r-RNA, yeast t-RNA, and poly(dA-dT)·poly(dA-dT) were obtained from Miles Laboratories, Inc.; CT-DNA from Calbiochem; and poly(dG-dC)·poly(dG-dC) from P-L Biochemicals.

Absorbance binding data were obtained on Cary 15 Spectrophotometer at 24°C in 5 cm cells. Chartreusin solutions at 1.6×10^{-5} M in 0.01 M phosphate buffer (pH 7.2) were titrated with small portions of concentrated polymer solutions and a chartreusin stock solution so that the concentration of chartreusin remained constant. The concentrations of the polymer stock solutions were calculated from the absorbance maxima using the following molar extinction coefficients: 6,200 for poly(dA-dT)·poly(dA-dT); 8,400 for poly(dG-dC)·poly(dG-dC); 6,600 for CT-DNA, 7,900 for yeast t-RNA; and 7,750 for r-RNA. The absorbance binding data at 420 nm were analyzed by various methods described in the text. The following molar extinction coefficients at 420 nm were used in the calculations: 12,700 for unbound chartreusin, and for totally bound chartreusin; 8,039 for r-RNA; 7,750 for t-RNA, and 7,230 for CT-DNA and the AT and GC polymers.

Results and Discussion

Visible Absorption Spectra

The visible absorption spectrum of chartreusin is dominated by two band maxima at 400 and 420 nm and two less intense bands which appear as shoulders near 385 and 445 nm (Fig. 2A). The addition of CT-DNA, yeast t-RNA, poly(dA-dT)·poly(dA-dT), poly(dG-dC)·poly(dC-dG), and *E. coli* 16s+23s r-RNA to solutions of chartreusin changes the absorption spectrum of the antibiotic as illustrated in

Fig. 3. Binding curves (A) and Scatchard plots (B) for chartreusin and the biopolymers studied in this work.

The solid lines represent values calculated from the binding parameters determined by least squares analysis.

△ t-RNA, ■ r-RNA, ● CT-DNA, □ GC polymer, ▲ AT polymer.

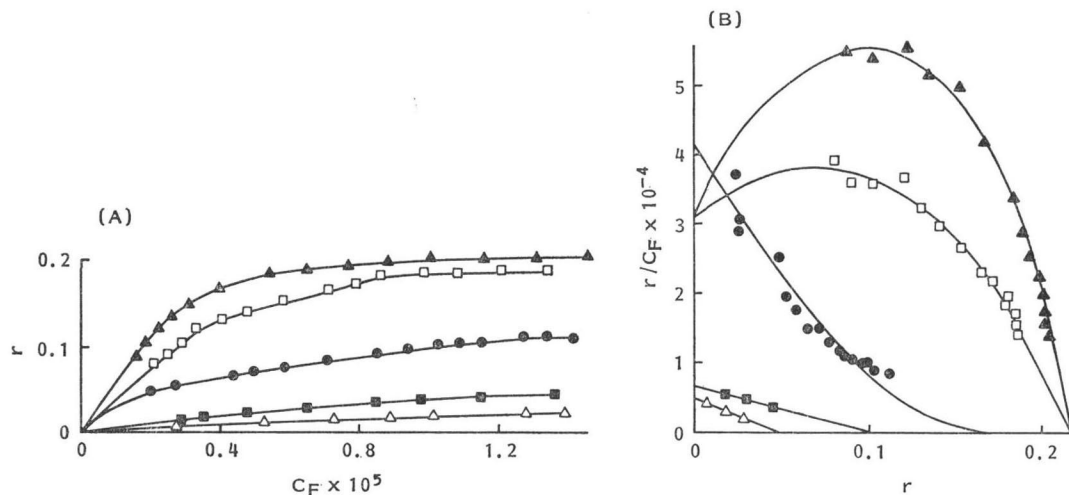


Table 1. Binding parameters determined by least squares analysis.

	Specific site model (SCHWARZ)				Site-exclusion (MCGHEE and VON HIPPEL)			
	$K_1 \times 10^{-4}$	w	$K_c \times 10^{-4}$	1/B	$K_1 \times 10^{-4}$	w	$K_c \times 10^{-4}$	1/B
AT polymer	10 ± 3	5.1 ± 0.9	50 ± 5	5 (Estimated)	3.1 ± 0.3	14.5 ± 1.5	45 ± 6	4.6 ± 0.04
GC polymer	15 ± 2	2.3 ± 0.2	34 ± 2	5 (Estimated)	3.1 ± 0.3	9.2 ± 1.5	28 ± 5	4.6 ± 0.1
CT-DNA		Not determinable			4.2 ± 0.2	1.000 (Assumed)	—	5.4 ± 0.3
r-RNA		Not determined			0.72 ± 0.02	1.000 (Assumed)	—	6.2 ± 0.3
t-RNA		Not determined			0.54 ± 0.02	1.000 (Assumed)	—	13.1 ± 0.9

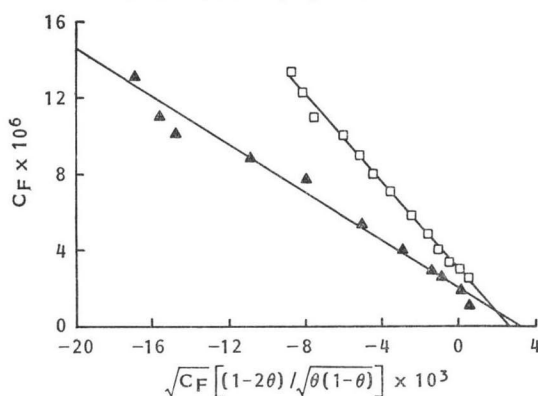
Fig. 2A for mixtures of CT-DNA and chartreusin. The absorption spectrum in the 350~450 nm region shifts to longer wavelengths and decreases in intensity, the shoulder absorption near 445 nm disappears, and isobestic points appear near 428 and 438 nm. These spectral changes are similar for all of the above polymers except that the concentration of polymer necessary to produce a given spectral change differs. This dependence of the absorption pattern on polymer is shown in Fig. 2B for polymer-chartreusin mixtures obtained at the same molar ratio of polymer-nucleotide to chartreusin of about 6.5.

Binding Isotherms and Scatchard Plots

The binding isotherms of r vs. C_F (r =molar ratio of bound chartreusin to polymer-nucleotide, C_F =free chartreusin concentration) and Scatchard plots are shown in Fig. 3. The horizontal nature of the CT-DNA, the AT polymer, and the GC polymer binding curves at large C_F values indicate about 0.2 bound chartreusin molecules per nucleotide for the AT and GC polymers and about 0.1 for CT-

Fig. 4. Plots from which the binding parameters were determined by linear regression analysis in the specific site model of SCHWARZ.

▲ AT polymer, □ GC polymer.



Analysis of the AT and GC Absorbance Data

For comparison purposes, the AT and GC polymer data can be analyzed according to the site-exclusion model of MCGHEE and VON HIPPEL⁹⁾ and SCHELLMAN¹⁰⁾ and the specific site model of SCHWARZ.¹¹⁾ To apply the specific site binding model of SCHWARZ requires that the number of binding sites per nucleotide or phosphate group, B , be estimated from a plot of C_F/C_T vs. C_N/C_T ; where C_F is the molar concentration of unbound chartreusin, C_T is the total molar concentration of chartreusin, and C_N is the total molar concentration of phosphate or nucleotide groups. The intercept on the C_N/C_T axis from the straight line determined from data at small values of C_N/C_T is $1/B$. The quantity θ is determined from B , C_N , and the molar concentration of bound chartreusin, C_B , according to: $\theta = C_B/C_N B$. A plot of C_F vs. $\sqrt{C_F}[(1-2\theta)/\sqrt{\theta(1-\theta)}]$ (from equation 31 of reference 11) should yield a straight line of slope $1/K_c w$ and C_F -axis intercept of $1/K_c$. In the expressions above, K_c is the cooperative binding constant, w is the cooperative binding parameter, and K_c/w is the intrinsic binding constant, K_1 . The C_F vs. $\sqrt{C_F}[(1-2\theta)/\sqrt{\theta(1-\theta)}]$ plots are shown in Fig. 4. The binding parameters and their errors (standard deviations) determined from the data of Fig. 4 by linear regression analysis and standard error propagation methods are given in Table 1.

The site-exclusion model of MCGHEE and VON HIPPEL was applied to the AT and GC data according to equation 15 of their publication.⁹⁾ (The "2w+1" term in this equation was corrected to "2w-1".) The parameters $1/B$, w , and K_1 were varied in a nonlinear regression analysis¹²⁾ to yield the results given in Table 1. The lines shown in the AT and GC Scatchard plots of Fig. 3B were calculated from the best fit parameters given in Table 1.

A row comparison of the AT and GC parameters given in Table 1 yields results attributable to the formulations inherent in each theory. Thus, the values of K_1 and w from the site-exclusion model are smaller and larger, respectively, than those from the specific site model. In addition, the values of K_1 and w for each polymer combine to yield nearly equal values of K_c . This behavior of the parameters is expected since in each theory, $1/K_c$ approaches the value of C_F at the midpoint of the binding curve (C_F vs. r) as w increases in magnitude.¹³⁾ A column comparison of the AT and GC data of Table 1 shows that K_c and w from both theories are greater for the AT polymer than for the GC polymer. The values of K_1 for a given theory are equal to within the calculated standard deviations.

DNA at saturation binding.

The Scatchard plots of r/C_F vs. r shown in Fig. 3B indicate a greater difference in the interaction of chartreusin with the polymers than do the binding curves of Fig. 3A. Only r-RNA and t-RNA show ideal straight-line Scatchard plots (all of the points are not plotted). The GC and AT polymers produce curves which have the unique shape associated with positive cooperative binding, while CT-DNA exhibits a curve having the opposite curvature. These binding data were analyzed by a number of models in the following sections. Binding parameters derived from these analyses are given in Table 1.

Analysis of the DNA-chartreusin Scatchard Data

The Scatchard plot of chartreusin with DNA is more difficult to analyze. The curvature of the plot could be attributed to multiple binding sites,¹⁴⁾ to specific site, negative-cooperative binding,¹⁴⁾ to site-exclusion binding,^{9,10)} to aggregation of free chartreusin,¹⁴⁾ to incorrect determination of the extinction coefficient of the bound chartreusin species (ϵ_B), or even to the nature of the DNA.¹⁵⁾ The quantity ϵ_B was determined by extrapolation techniques¹⁴⁾ at moderate nucleotide/chartreusin molar ratios (10~30) and also from large molar ratios (50~100) (total binding). The two values of ϵ_B were identical to within experimental error, $\epsilon_B=7,228$ and $7,276$, and so we considered ϵ_B to be well determined. We did not evaluate the effect of CT-DNA type on the Scatchard plot and found no evidence for free chartreusin aggregation at ten times the concentration of the interaction experiments. The binding data could not be analyzed according to the specific site, negative-cooperative binding model of SCHWARZ since a straight-line plot based on equation 31 (see Fig. 4) was not obtained. Attempts to fit the data to a model with two affinity constants and two stoichiometry parameters were unsuccessful. This leaves the site-exclusion binding model to consider.

Attempts to analyze the chartreusin-DNA data with the site-exclusion model of MCGHEE and VON HIPPEL⁹⁾ (their equation 15) were unsuccessful. Depending on the initial estimates, the K_1 , $1/B$, and w parameters either did not converge to meaningful values, had very large standard deviations, or both. The results suggested we decrease the number of parameters. This was done by fitting the data to the non-cooperative ($w=1$) binding model (equation 11 of reference 9). Convergence was obtained in this analysis to yield the calculated parameters and standard deviations given in Table 1. The Scatchard curve calculated from these parameters is presented as the line through the chartreusin - CT-DNA data in Fig. 2B.

For comparison purposes, the straight-line Scatchard data for t-RNA and r-RNA were treated in the same way as those for CT-DNA. The binding parameters from this analysis are shown in Table 1. Analysis of the t-RNA and r-RNA data according to standard Scatchard methods would yield binding constants $1/B$ times greater than those shown in Table 1.⁹⁾

Discussion of the Binding Data

Based on the magnitudes of the intrinsic binding constants given in Table 1, the order of binding affinity is: CT-DNA > AT polymer ~ GC polymer > r-RNA > t-RNA. However, since the binding of chartreusin to the AT and GC polymers is cooperative, the binding constant for these polymers at sites adjacent to bound chartreusin molecules is much greater than the intrinsic binding constant (w times as great for one neighbor). Based on the cooperative binding constants for these polymers and the intrinsic binding constants for the other polymers, the order of binding affinity is as follows: AT polymer ~ GC polymer > CT-DNA > r-RNA > t-RNA. This order agrees better with the absorbance data of Fig. 2B than the previous binding order since, according to Fig. 2B, the AT and GC polymers shift the chartreusin spectrum further towards that of the bound-species spectrum than does CT-DNA (at a given molar ratio of nucleotide to chartreusin). Furthermore, the latter binding order is also in better agreement with our findings that the induced CD spectra for the AT and GC polymers are significantly greater than that for CT-DNA.⁶⁾

The reason why chartreusin binds cooperatively to the AT and GC polymers but not to CT-DNA is unclear. One possible explanation might be that chartreusin binds with high affinity to alternating pyrimidine-purine base pair sequences 2 or 3 base pairs in length (as suggested by the binding data of Table 1) and with low affinity to other sequences. In this case, chartreusin molecules would be in close proximity on the AT and GC polymers for cooperative interaction to occur. The probability of these

high affinity sites appearing adjacent to one another in CT-DNA would be small (assuming a random distribution of bases). Hence, chartreusin would not bind cooperatively to CT-DNA. This explanation is consistent with a recent study which suggests that chartreusin binds specifically to 5'-CGC-3' sequences.⁸⁾ Our results suggest that chartreusin binds with high affinity to alternating AT sequences as well. Additional studies are necessary to clarify the base pair specificity of chartreusin.

References

- 1) LEACH, B. E.; K. M. CALHOUN, L. E. JOHNSON, C. M. TEETERS & W. G. JACKSON: Chartreusin, a new antibiotic produced by *Streptomyces chartreusis*, a new species. *J. Am. Chem. Soc.* 75: 4011~4012, 1953
- 2) SIMONITSCH, E.; W. EISENHUTH, O. A. STAMM & H. SCHMID: Über die Struktur des Chartreusin. *Helv. Chim. Acta.* 43: 53~63, 1960
- 3) BHUYAN, B. K.; H. E. RENIS & C. G. SMITH: A collagen plate assay for cytotoxic agents. II. Biological studies. *Cancer Res.* 22: 1131~1136, 1962
- 4) MCGOVREN, J. P.; G. L. NEIL, S. L. CRAMPTON, M. I. ROBINSON & J. D. DOUROS: Antitumor activity and preliminary drug disposition studies on chartreusin (NSC 5159). *Cancer Res.* 37: 1666~1672, 1977
- 5) KONISHI, M.; K. SUGAWARA, M. TSUNAKAWA, Y. NISHIYAMA, T. MIYAKI & H. KAWAGUCHI: BMY-28090, a new antitumor antibiotic related to chartreusin: Isolation, chemistry and activity. Abstracts of 14th Int. Cong. Chemother. P-17-13, p. 320, Kyoto, June 23~28, 1985
- 6) LI, L. H.; T. D. CLARK, L. L. MURCH, J. M. WOODEN, L. M. PSCHIGODA & W. C. KRUEGER: Biological and biochemical effects of chartreusin on mammalian cells. *Cancer Res.* 38: 3012~3018, 1978
- 7) YAGI, M.; T. NISHIMURA, H. SUZUKI & N. TANAKA: Chartreusin, an antitumor glycoside antibiotic, induces DNA strand scission. *Biochem. Biophys. Res. Commun.* 98: 642~647, 1981
- 8) URAMOTO, M.; T. KUSANO, T. NISHIO, K. ISONO, K. SHISHIDO & T. ANDO: Specific binding of chartreusin, an antitumor antibiotic, to DNA. *FEBS Lett.* 153: 325~328, 1983
- 9) MCGHEE, J. D. & P. H. VON HIPPEL: Theoretical aspects of DNA-protein interactions: Cooperative and non-cooperative binding of large ligands to a one-dimensional homogeneous lattice. *J. Mol. Biol.* 86: 469~489, 1974
- 10) SCHELLMAN, J. A.: Cooperative multisite binding to DNA. *Isr. J. Chem.* 12: 219~238, 1974
- 11) SCHWARZ, G.: Cooperative binding to linear biopolymers: I. Fundamental static and dynamic properties. *Eur. J. Biochem.* 12: 442~453, 1970
- 12) METZLER, C. M.; G. K. ELFRING & A. J. MCEWEN: A package of computer programs for pharmacokinetic modeling. *Biometrics* 30: 562~563, 1974
- 13) SCHNEIDER, F. W.; C. L. CRONA & S. K. PODDER: Cooperative binding to a one-dimensional lattice. The amylose-iodine-iodide complex. *J. Phys. Chem.* 72: 4563~4568, 1966
- 14) BLOOMFIELD, V. A.; D. M. CROTHERS & I. TINOCO, Jr.: *Physical Chemistry of Nucleic Acids.* pp. 406~420, Harper and Row, New York, 1974
- 15) KRUEGER, W. C.; L. M. PSCHIGODA, S. L. F. SCHPOK, A. MOSCOWITZ, J. P. MCGOVREN, P. NETA, M. V. MERRITT & L. H. LI: The interaction of nogalamycin and analogs with DNA and other biopolymers. *Chem. Biol. Interact.* 36: 1~18, 1981